

TESTING OF A COCURED COMPOSITE FRAME PANEL BY THE APPLICATION OF VACUUM AS AN ALTERNATE TO FRAME BENDING TEST

Kotresh M Gaddikeri¹, Viswamurthy S R¹, Viswarupachari CH¹, Dinesh B L¹,
Rueben Dinakar² and Sven H Werner³

¹ CSIR-National Aerospace Laboratories, Bengaluru, India; kotresh@nal.res.in

² Airbus Group India Pvt Limited, Bengaluru, India

³ AIRBUS Operations GmbH, Hamburg, Germany

Abstract: The Frame Bending Test (FBT) of fuselage panels is plagued by complex design at load introduction regions, high workload for assembly of specimen to test rig and the need for disassembly for access to stiffened structure. An alternative to the FBT was explored by the application of vacuum on skin side of panel using a metallic fixture while frame side of panel is subjected to atmospheric pressure. The vacuum level can be controlled to obtain the desired differential pressure. A curved composite panel was designed with three cocured corrugated frames and eight stringers under the INFUSE (Integral Fuselage Shell Concepts) Project between CSIR-NAL and Airbus. The shear clips, to stabilise the frame web laterally, were eliminated by the corrugation of web. A metallic fixture was developed to mount the panel to enable application of vacuum. Finite element (FE) analysis of panel mounted on fixture was carried out to understand the structural response. The desired circumferential strains in panel were achieved by the proper sizing of vacuum fixture. Panel response was monitored using dial gages, strain gauges and Digital Image Correlation (DIC). Acoustic emission was also monitored during the test. Through use of vacuum pumps, pressure on the skin side was reduced to 20mbar and panel withstood the differential pressure successfully. Ultrasonic scan carried out on cocured joints showed no disbonds. The proposed Vacuum test has advantages like smooth and uniform load introduction, quick assembly and reduced cost. It also allows quick access to specimen for DIC, non-destructive inspection and other sensors on frame side during the test and presents itself as an alternate to FBT.

Keywords: Frame bending test; Vacuum loading; Digital image correlation; Corrugated frame;

INTRODUCTION

Fuselage panels in pressurized cabins are subjected to differential pressure loads in addition to inertia loads. Structural integrity of stiffened fuselage panels is routinely checked under application of frame bending loads (Figure 1) [1]. In this work, we explore an alternative to the frame bending test by directly applying a differential pressure load to the curved panel. In this approach, vacuum is applied on the skin side of the composite fuselage panel while the frame side of the panel is subjected to ambient pressure. The extent of vacuum is controlled to obtain desired level of differential pressure between the

two sides of the panel. To realize vacuum loading of the curved composite panel, a fixture is designed to support the panel. This vacuum testing methodology was used by CSIR-NAL successfully on previous programs for testing of composite parts.

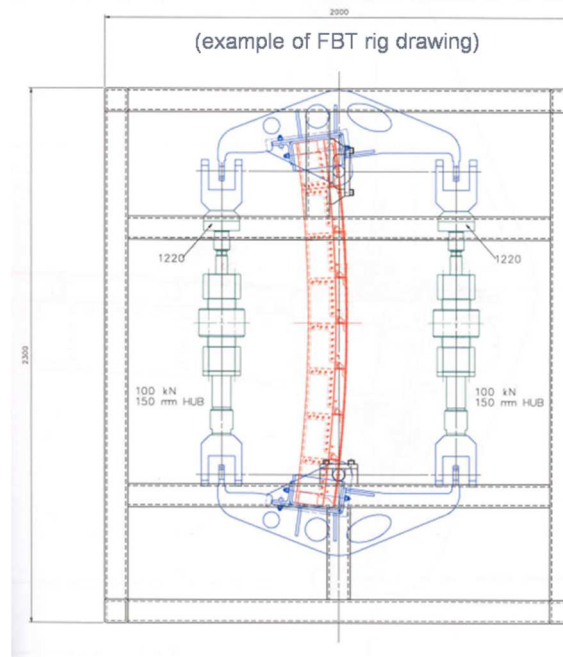


Figure 1: Schematic of frame bending test [1]

Cocured Composite Frame Panel

Figure 2 shows the curved composite panel as a part of Airbus INFUSE demonstrator project. The curved panel is fabricated using autoclave molding process using AS4/914 Carbon/epoxy UD prepreg supplied by Hexcel®. The skin, stringers and frames are co-cured. A novel feature of this panel is the absence of shear clips which are traditionally used to stabilize the frame webs. Instead, the frame web is corrugated to improve its resistance to buckling (Figure 2). The radius of curvature of the panel is 1890 mm and the length of the panel is 1905 mm. The stringer spacing and frame spacing are 170 mm and 635 mm, respectively. The panel contains three corrugated frames and eight stringers.

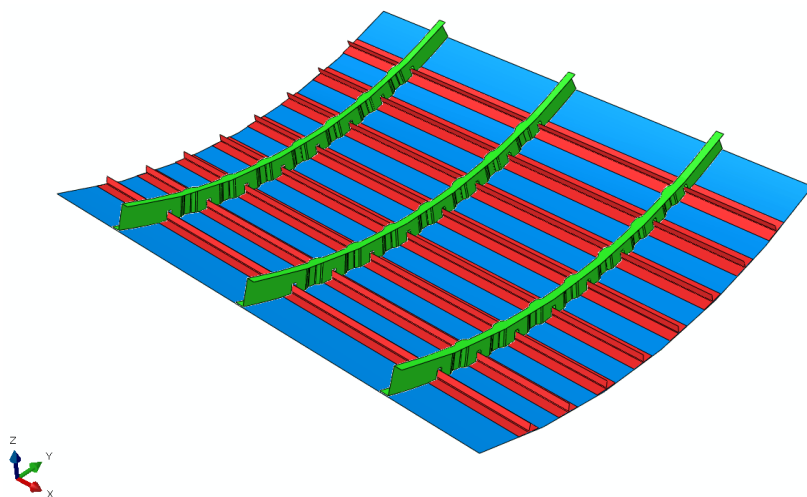


Figure 2: Composite curved panel with cocured skin, stringers and frames

VACUUM TEST FIXTURE

The fixture is of C-shaped cross section running along the periphery of curved panel. The bottom flange of fixture is fixed to a rigid granite surface table. The composite panel is fastened along its edges to the top flange of fixture at regular intervals. The air enclosed between the interior of the fixture and skin surface of curved panel is evacuated using a vacuum pump thereby creating the differential pressure. The magnitude of differential pressure can be adjusted by partial evacuation of air in the cavity. The main design driver of the support fixture is its stiffness. The fixture should be stiff enough such that it undergoes low deformations under maximum vacuum loading. As the curved panel skin is very thin compared to its radius, the stiffness of fixture plays an important role in the development of membrane forces in the curved panel in hoop direction. The stiffness of fixture could be tailored to attain the desired strain levels for a given vacuum loading in composite panel, particularly in the hoop direction.

The fixture is made up of 10 mm thick mild steel material with two gussets on each of the channel along its length (Figure 3). The fixture is fastened to a rigid granite surface plate all along its periphery with the help of fasteners. To estimate strains in the skin and frames under vacuum loading, a finite element model of the composite panel was developed using Abaqus platform [2]. Figure 4 shows the FE model of the composite panel and the test fixture.

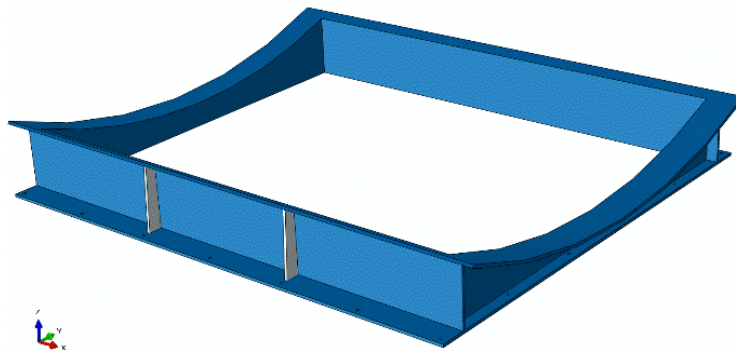


Figure 3: Vacuum test fixture

The curved panel is meshed with two dimensional, 4-noded shell elements in Abaqus (S4R) and the fixture is modelled using three dimensional 4-noded linear tetrahedron (C3D4) elements. The typical element size used for shell elements is 15 mm and 10 mm for tetrahedron elements. Figure 4 shows the entire assembly of composite curved panel and vacuum testing fixture. To represent the joints between skin, stringers and frames in finite element modelling, the tie constraint option in Abaqus is used [2]. A tie constraint ties two separate surfaces together so that there is no relative motion between them. This enables the applied load transfer from one part to another part. In tie constraint definition, one surface in the constraint is designated to be the slave surface and the other surface is the master surface. Table 1 gives the details of various tie constraints used in the present FE model along with master and slave surface information.

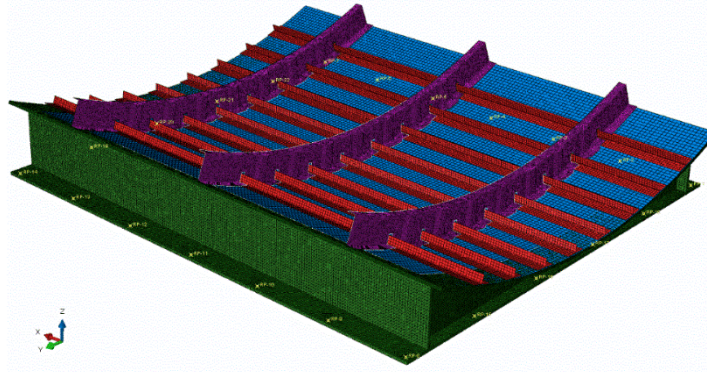


Figure 4: Finite element model of panel and test fixture

Table 1: Tie constraints information in the curved panel assembly

Tie constraint	Master surface	Slave surface
Skin-Stringers	Skin top surface	Stringer flange bottom surface
Stringers -Frame	Stringer flange top surface	Frame flange bottom surface
Skin- Frame	Skin top surface	Frame flange bottom surface
Skin-Fixture	Fixture flange top surface	Skin bottom surface

In the analysis, the bottom flange of the fixture is completely constrained at all 22 fastener locations. A tie constraint is imposed between the curved panel and fixture to simulate large number of bolts provided at very close intervals. One bar differential pressure load is applied to panel skin surface and internal faces of the fixture. A linear static analysis is carried out in Abaqus/Standard [2].

Figure 5 shows the skin strain in hoop direction under 1 bar vacuum loading. Maximum strains are observed between Frame-1 and Frame-3 ranging from 1000 to 2200 $\mu\epsilon$ in tension. Figure 6 shows the strain along middle frame top flange length in the hoop direction. These strains are extracted at 15 mm from the edge of the flange. In the middle of the frame, strains range between 3500 to 4500 $\mu\epsilon$ in compression under 1 bar vacuum loading. The strain levels in the skin and frame was acceptable and hence the fixture design was frozen and fabrication was initiated.

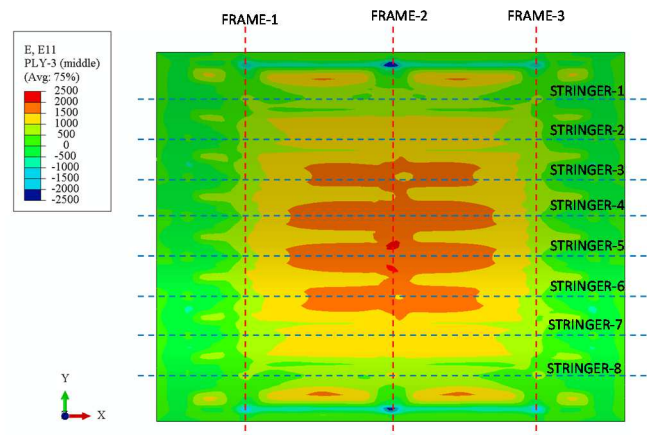


Figure 5: Skin strains in hoop direction under 1 bar vacuum load

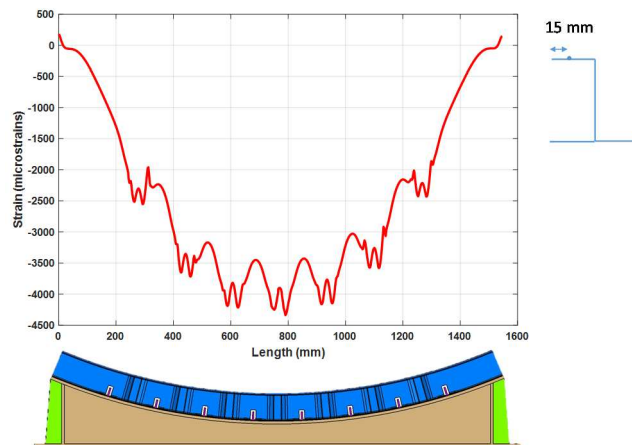


Figure 6: Strains (hoop direction) along middle frame top flange length

VACUUM TESTING OF THE PANEL

In order to apply vacuum loading to the panel, a vacuum bag is applied along the periphery of the panel. The air enclosed between the interior of the fixture and exterior surface of curved panel (outer skin surface) is evacuated using a vacuum pump thereby creating the differential pressure (Figure 7). The magnitude of differential pressure can be adjusted by partial evacuation of air in the cavity. A servo controller is used to control the vacuum. During vacuum testing, pressure inside the bag is reduced in steps of 100 mbar starting from ambient pressure (approximately 913 mbar at Bengaluru). After reaching desired vacuum level, the panel is unloaded gradually again in steps of 100 mbar until pressure inside the bag reached ambient pressure. During both loading and unloading conditions, strain gauges, dial gages, full field deformations using DIC and Acoustic emission (AE) sensors are monitored. Figure 7 also shows the panel with strain gauges, dial gages and DIC speckling to carryout full field strain measurement. Two AE sensors were bonded to the panel (Figure 8a). These AE sensors are placed to detect the onset of damage during the loading of panel.

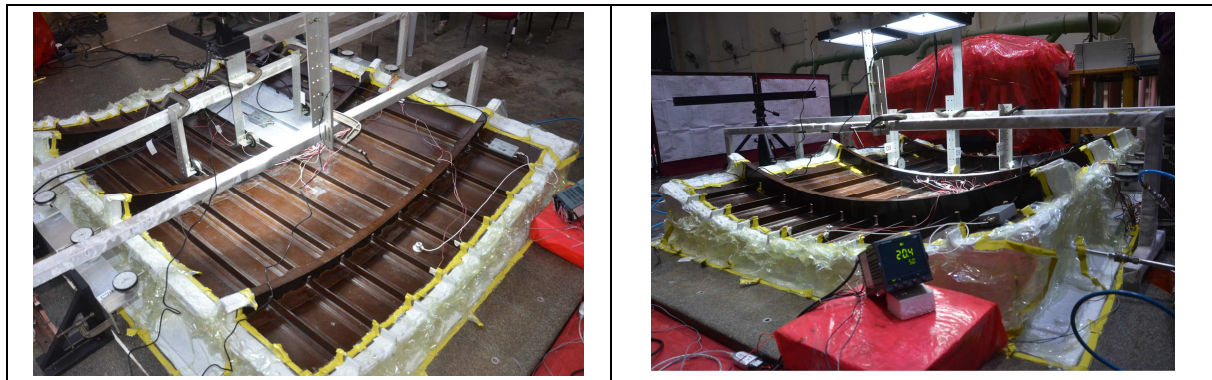


Figure 7: Vacuum test setup

Test-1: Vacuum loading up to 100mbar pressure

During Test-1, the pressure inside the vacuum bag was reduced gradually to 100 mbar. When the pressure was further reduced to 95 mbar, high acoustic activity was observed by the acoustic sensors and further loading was stopped. The panel was completely unloaded in steps again and ultrasonic C-scan was carried out on the skin-frame and skin-stringer interfaces. Figure 8b shows the acoustic activity recorded during the test. AE data indicated that no valid AE activity occurred up to pressure of 400 mbar. Between 400 to 100 mbar, AE activity is discrete and less number of hits and most of amplitude < 55 dB indicating damage initiation. At 100 mbar pressure, AE has continuous activity with higher number of hits and counts. Clustering of hits with amplitudes between 48-60 dB. Hits are also seen up to 95dB indicating rapid growth of localized defects formed earlier.

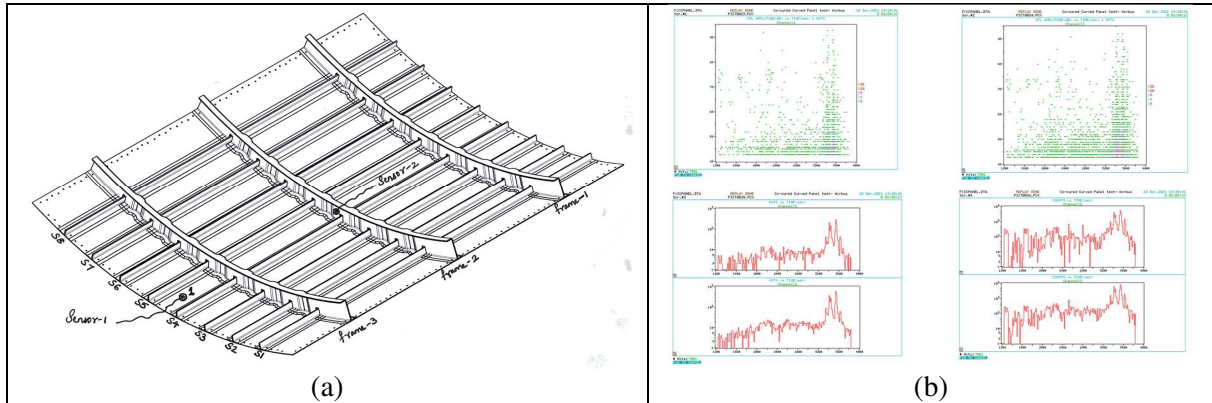


Figure 8: (a) AE sensors attached to panel (b) Acoustic activity during Test-1

Figure 9 shows the defects observed by ultrasonic A-scan conducted after Test-1. This figure highlights both (i) Defects after manufacturing and (ii) Defects observed after Test-1. The vacuum loading has resulted in disbands between frame and stringer near mouse-hole junctions adjacent to the fixture (majority of disbands at the cross over of stringer 1-Frame 2 and stringer 8- Frame 2). Some defects were also found in frame web region near mouse hole at the same cross overs (an extension of the disbond between stringer and frame interface). It was decided to load the panel again after installing rivets locally to prevent further growth of disbands. A total of 29 blind rivets were installed at skin-stringer-frame interfaces and at skin-frame interfaces.

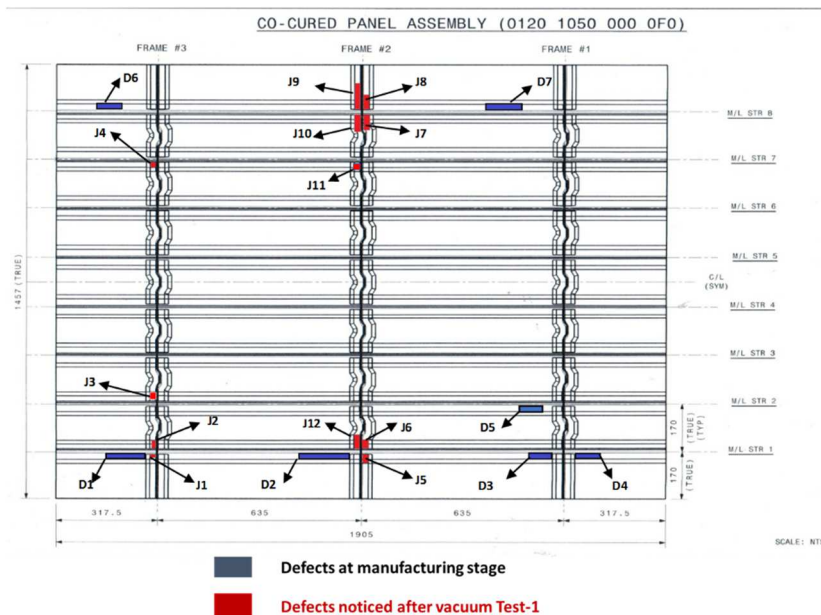


Figure 9: Defects observed in the panel from ultrasonic A-scan after Test-1

Test-2: Vacuum loading up to 20mbar pressure

After installation of rivets, vacuum loading was carried out again. During Test-2, DIC cameras were focused on Frame-2 top flange for monitoring its deformations and strains (Figure 10). Dial gages were mounted to monitor out-of-plane deformation of Frame-2 web (Figure 10). The pressure inside the vacuum bag was reduced gradually from ambient pressure (913 mbar) to 20 mbar. No acoustic activity was observed by the AE sensors. Further reduction in pressure inside the vacuum bag below 20mbar was not possible and panel was gradually unloaded back to ambient pressure. All monitoring systems i.e. strain gauge, dial gage and DIC acquired data during both loading and unloading of the panel. In the following plots, wherever applicable, data from both Test-1 and Test-2 have been combined for easy and quick comparison. Prediction from FE analysis is also added to the plots, wherever possible.

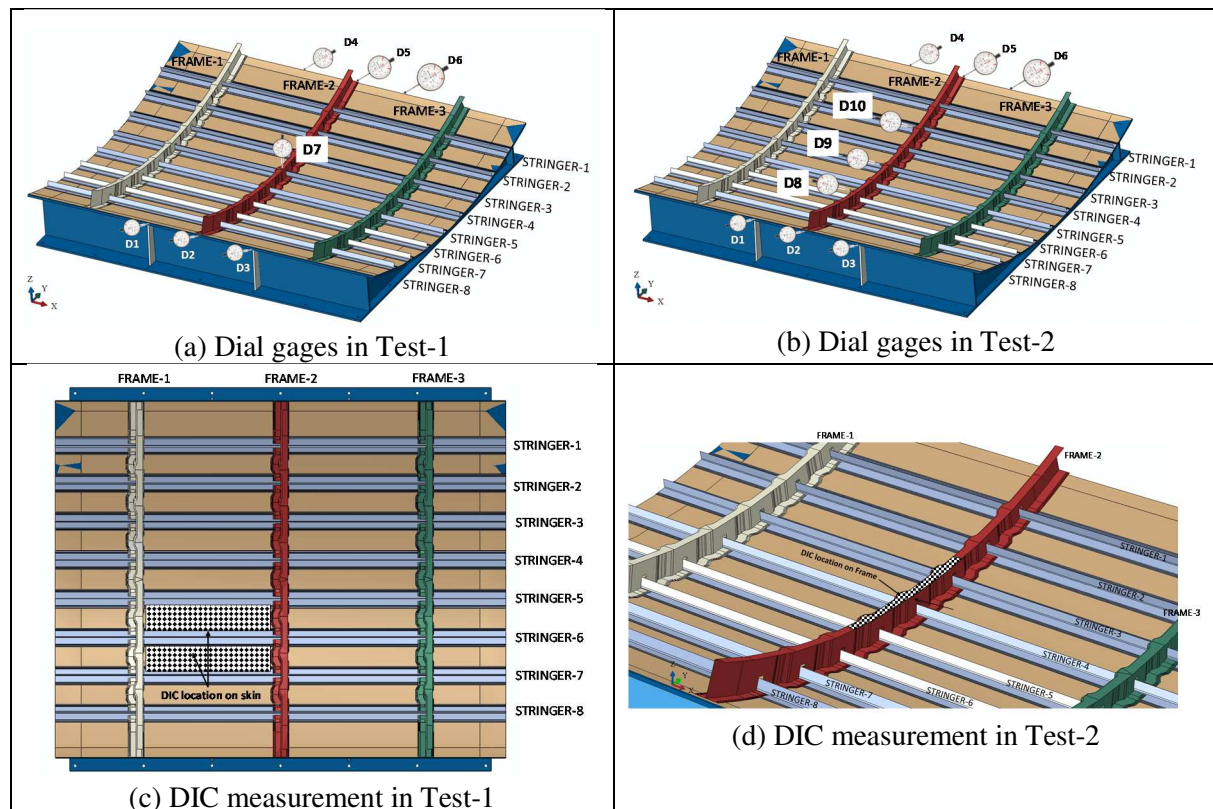


Figure 10: Dial gage and DIC measurement locations during vacuum tests

Figure 11 shows the lateral deformation of test fixture due to vacuum loading. At maximum vacuum, measured fixture deformation is 3.2mm while deformation predicted by FE analysis is 3.0mm. Figure 12 shows the lateral and out-of-plane deformations of Frame-2 top flange at 20 mbar measured using DIC. Figure 13 shows the out-of-plane deformation of Frame-2 in tests and analysis. At maximum load, frame deformation in test was 16.6mm and numerical prediction is 14.7mm. Figure 14 to Figure 18 show the strains at various locations in the panel. These plots show that there is good agreement between test and numerical simulation for overall response of panel and test fixture.

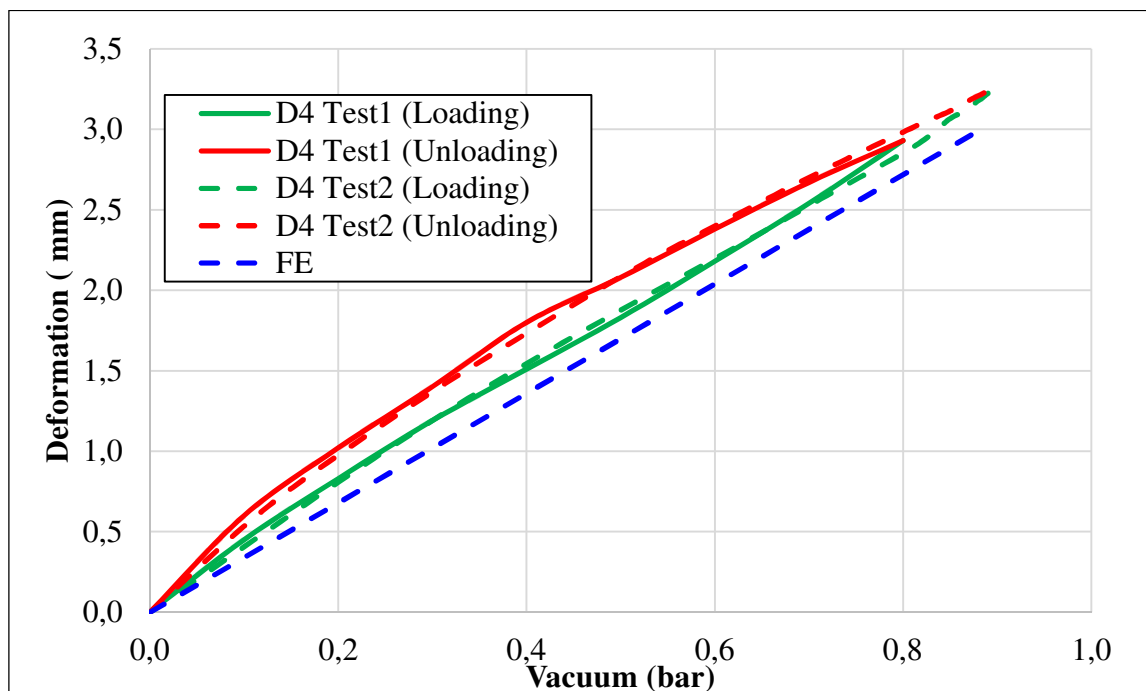


Figure 11: Lateral cave-in response of fixture (Dial gage 4)

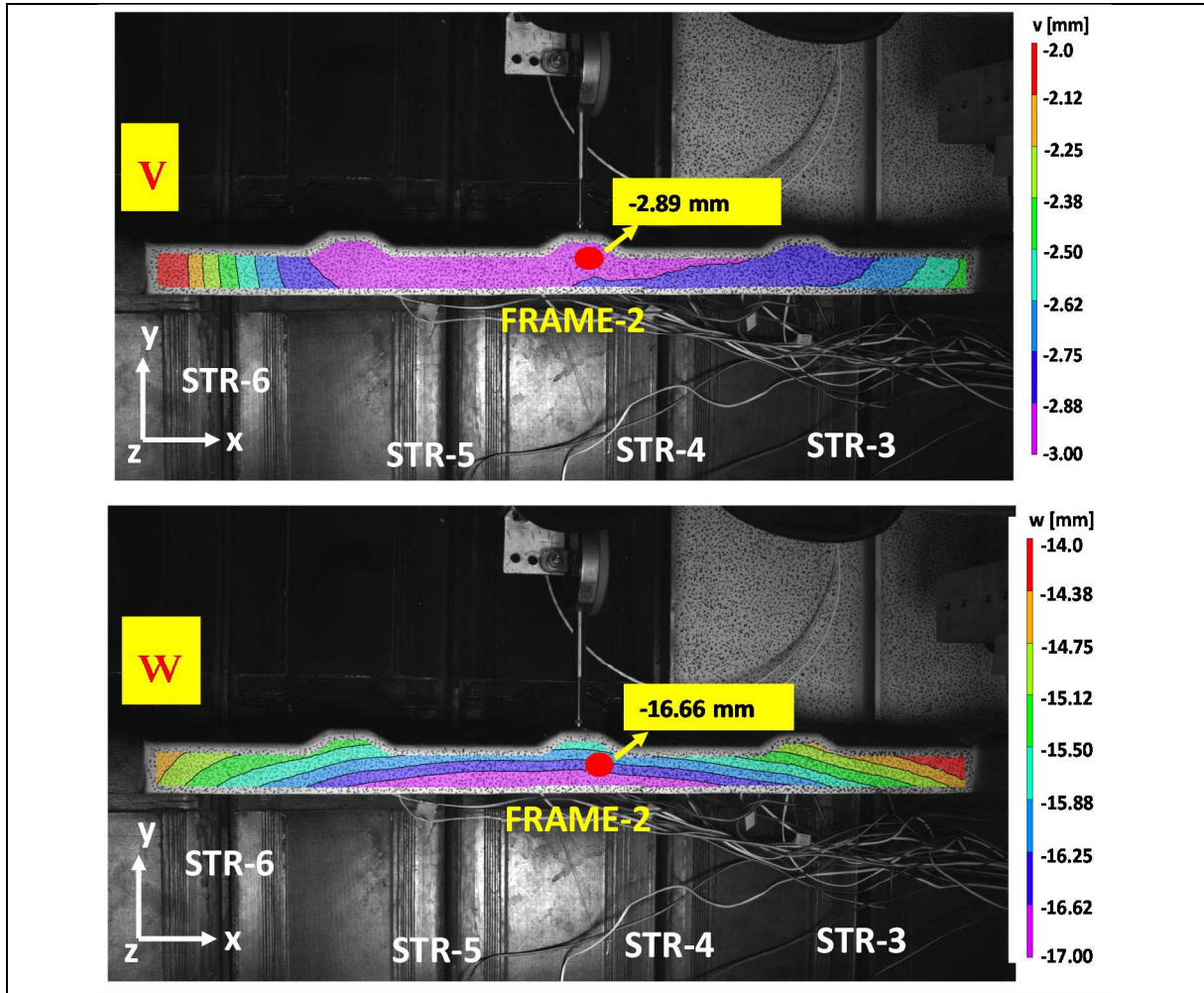


Figure 12: Lateral and Out-of-plane deformations of Frame-2 top flange at 20 mbar (DIC)

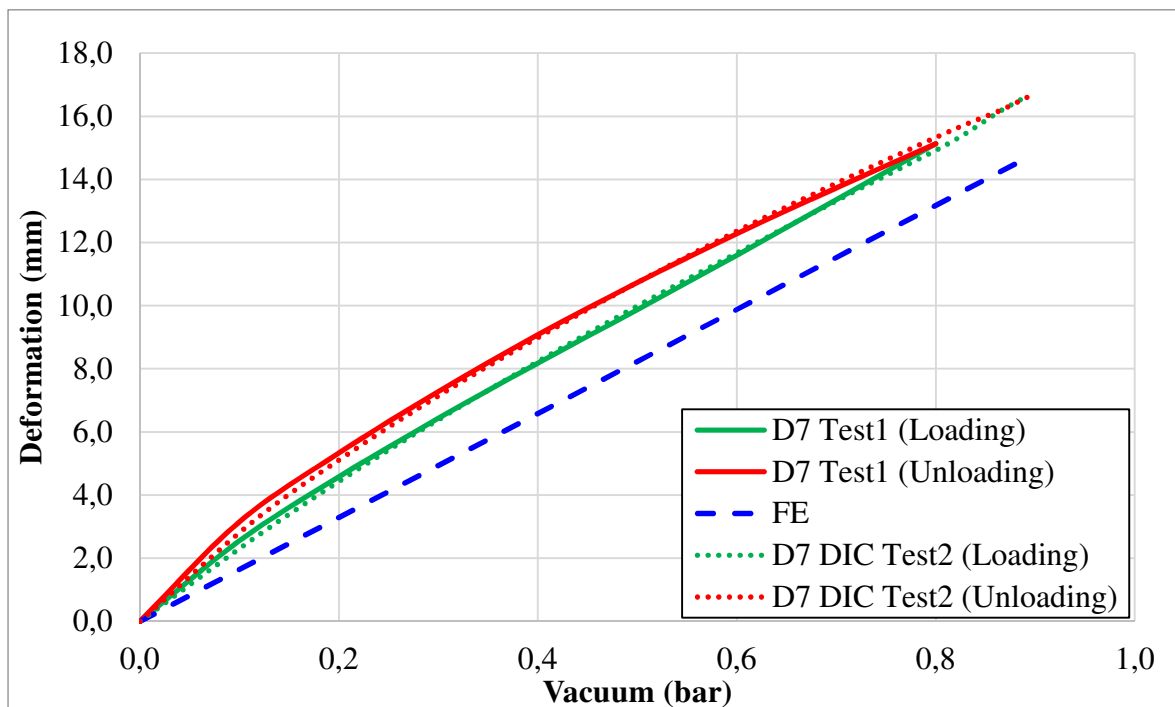


Figure 13: Out-of-plane deformation of Frame-2 (Dial gage 7)

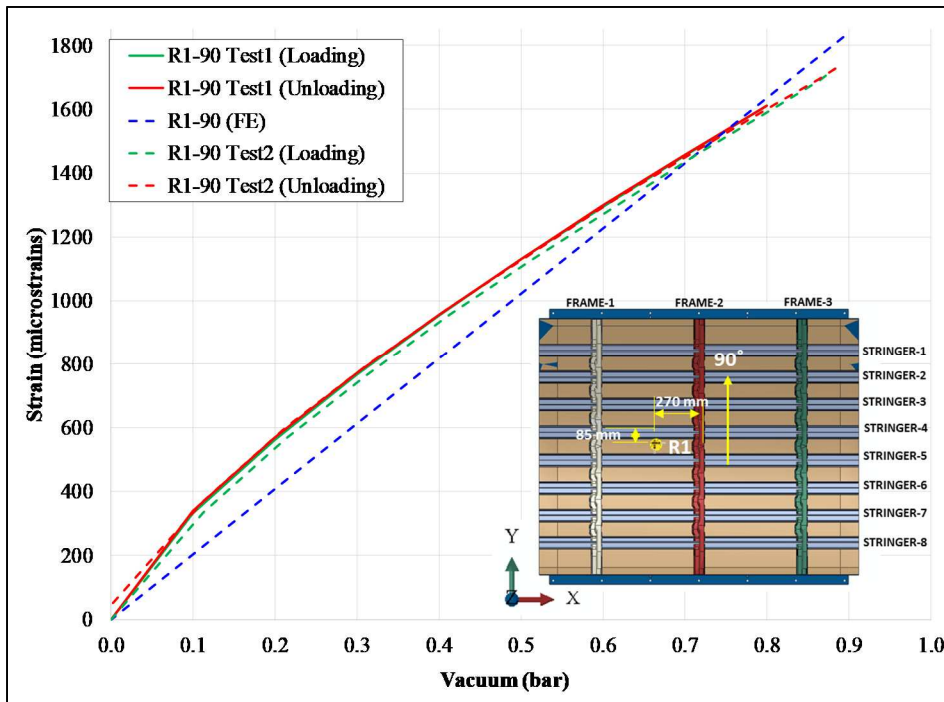


Figure 14: Skin strain gauge R1(90)

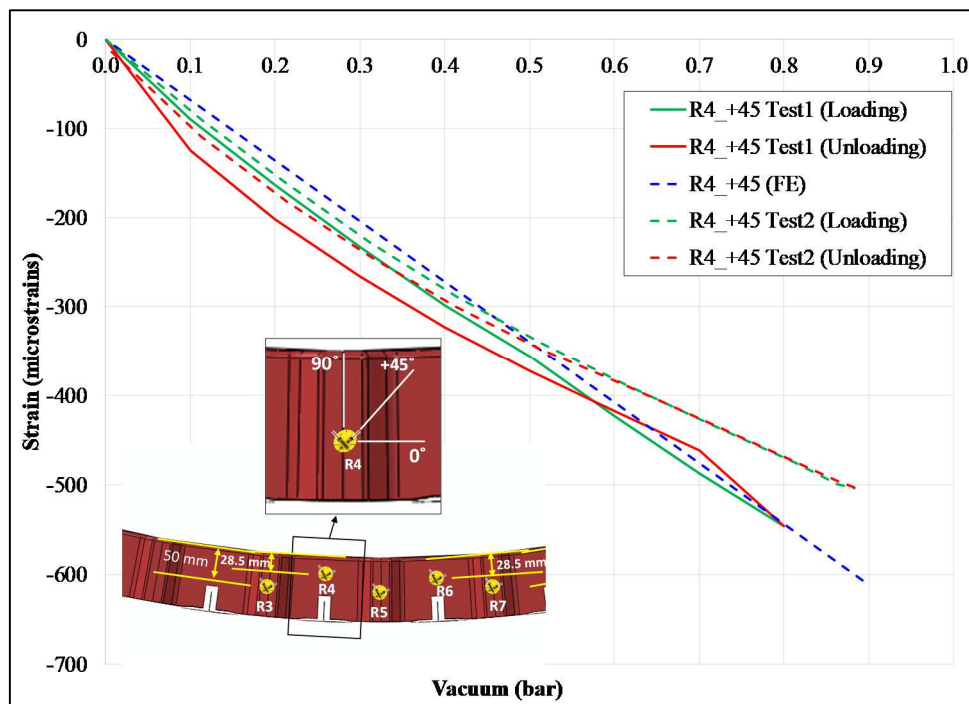


Figure 15: Frame-2 web strain gauge R4(+45)

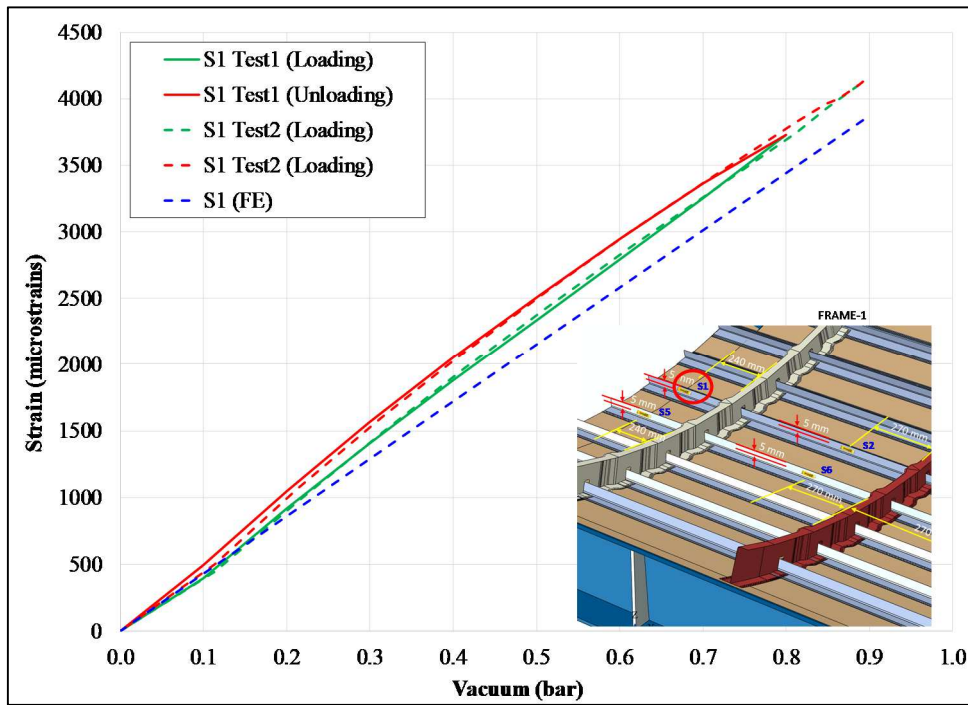


Figure 16: Stringer-4 web strain gauge S1

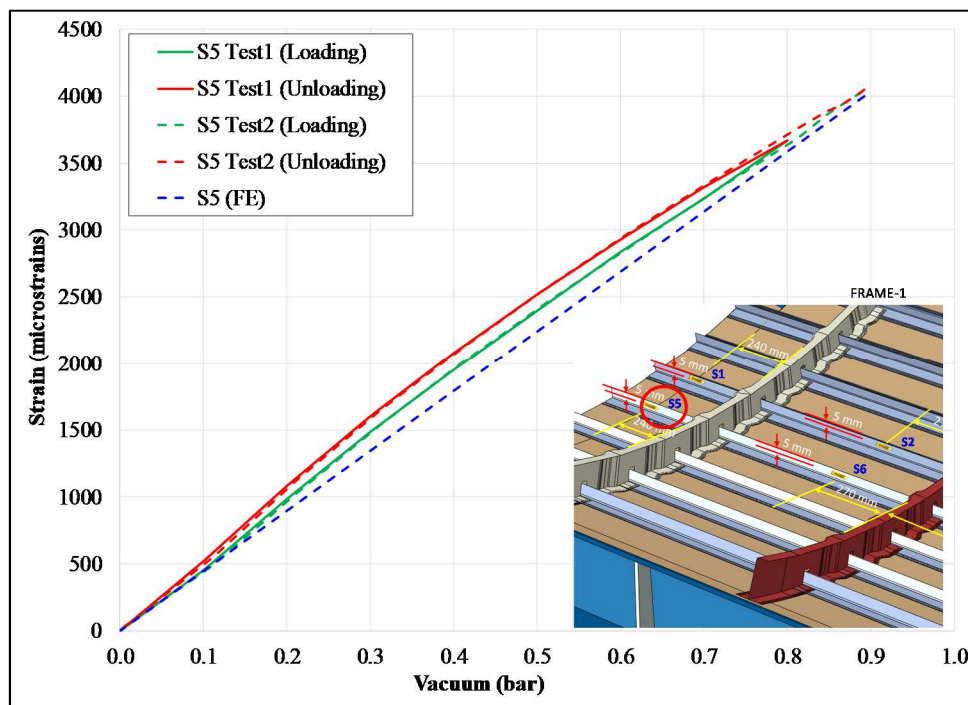


Figure 17: Stringer-5 web strain gauge S5

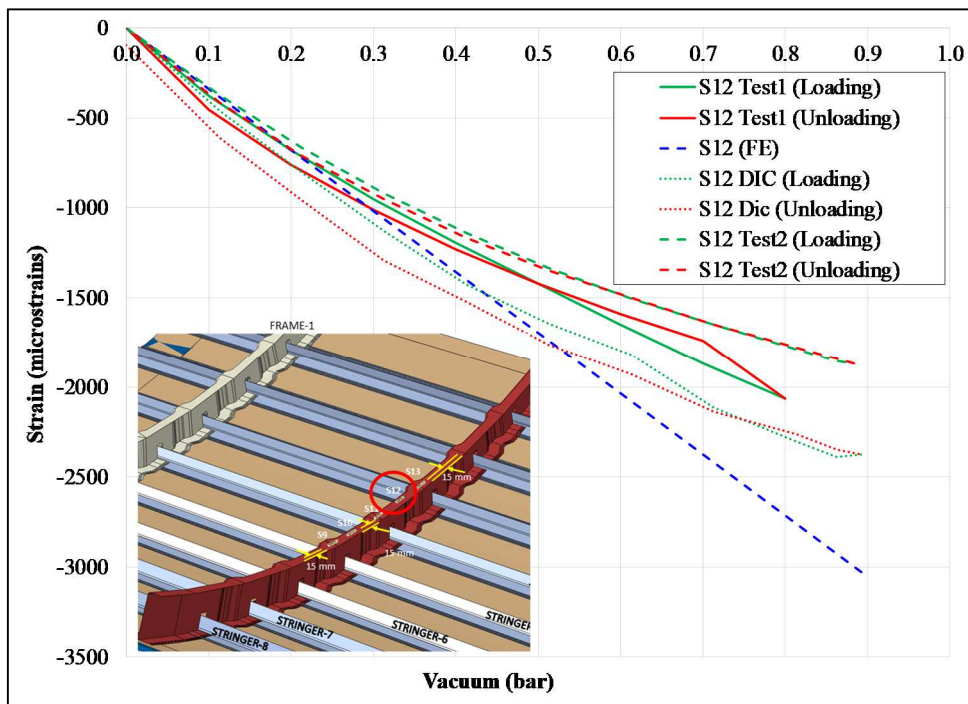
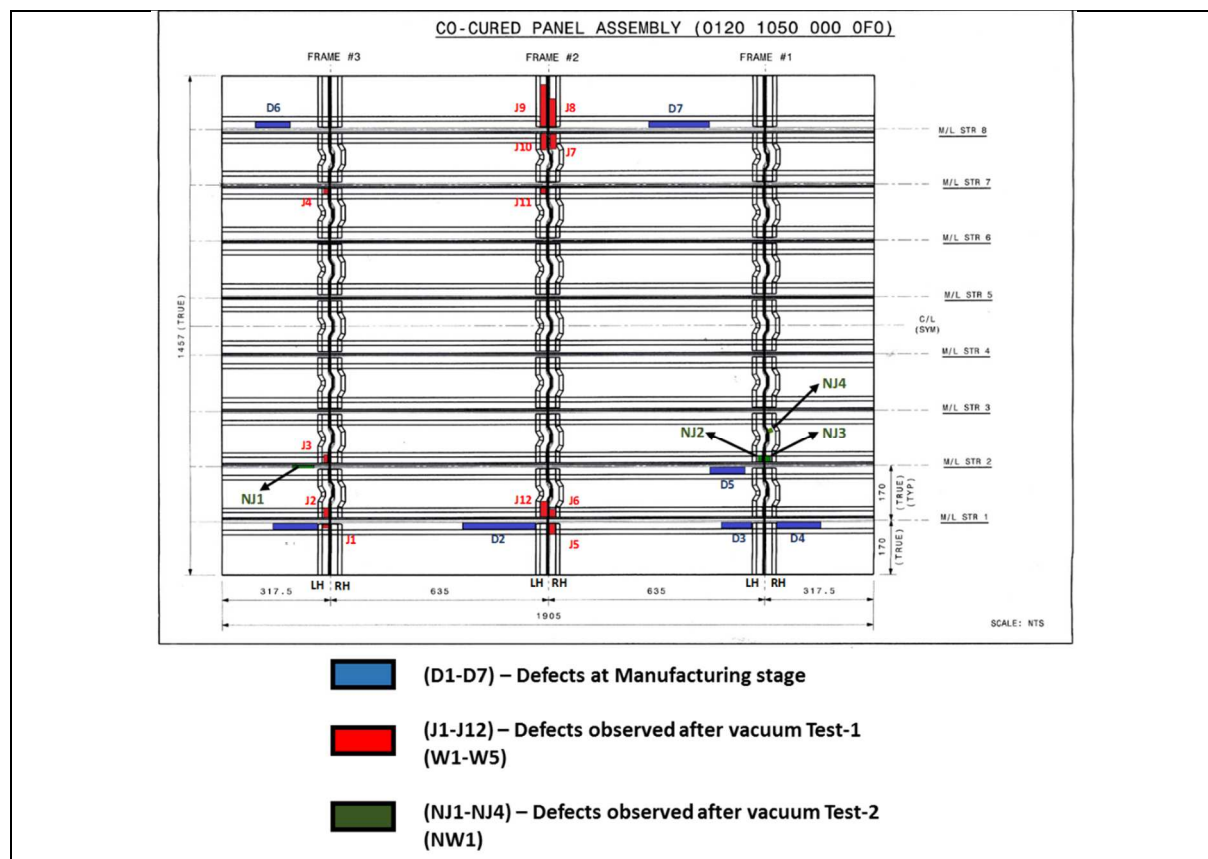


Figure 18: Frame-2 top flange strain gauge S12

Figure 19 shows the defects observed by ultrasonic A-scan conducted after Test-2. This figure shows (i) Defects after manufacturing stage, (ii) Defects observed after Test-1 and (iii) Additional defects observed after Test-2. It is seen that defects observed at manufacturing stage did not grow during Test-2. Also, installation of rivets after Test-1 on the stringer and frame interfaces arrested growth of disbonds observed after Test-1. After Test-2, four new delaminations were found in stringer and frame flanges and one new delamination in frame web.



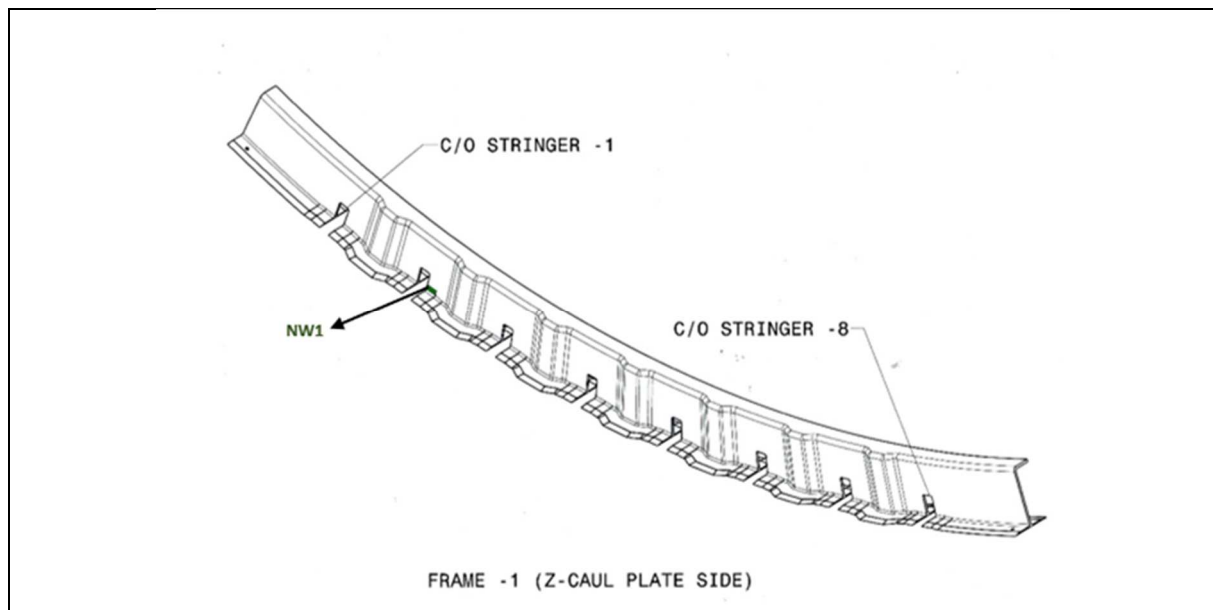


Figure 19: Defects observed in the panel from ultrasonic A-scan after Test-2

CONCLUSIONS

A metallic fixture was developed to mount the panel to enable application of vacuum. Finite element analysis of panel mounted on fixture which in turn was fixed to a rigid granite plate was carried out to understand the structural response. It was found that the circumferential strains are affected by the lateral stiffness of the fixture. The desired circumferential strains in the panel were achieved by proper sizing and support system of the vacuum fixture. The location of strain gauges, DIC regions and dial gauges were finalized based the results of FE analysis. Acoustic Emission was also monitored during the test.

Two vacuum tests were carried out on the panel and pressure inside the cavity was gradually reduced to 100 mbar and 20mbar in Test-1 and Test-2, respectively. Structural responses were measured both during loading and unloading for each load step. The first test was stopped at 100mbar vacuum pressure because of AE activity. Post-test ultrasonic scan of cocured joints showed the disbonds in the frame and stringer crossover regions in proximity to metallic fixture. Rivets were installed on disbonds to prevent further growth. The second test was done and panel was loaded up to 20mbar and panel withstood the vacuum pressure successfully. The structural response in terms of deflections and strains were correlated with numerical simulations. The repeatability of structural response was seen between the two tests and no permanent deformation was noticed after the removal of vacuum. An alternate method to frame bending test using the application of vacuum on a cocured fuselage panel was successfully demonstrated.

ACKNOWLEDGEMENTS

Authors acknowledge the support of staff of CSIR-NAL towards execution of this research. Authors thank Dr.Ramesh Sundaram, Dr.Ramesh Kumar M, Mr.Vinayak Patil, Mr. Sanjeev Kumar, Mr.V.Srinivasa, Mr.Amit Kumar Gupta, Mr.M.Siva, Mr.Kailash Singh, Mr.Kamboji Prakash and Mr.Praveen Kumar JN for their assistance in carrying out the vacuum test and contributions.

REFERENCES

- [1] Plokker, M.; Daverschot, D.; Beumler, T.: Hybrid Structure Solution for the A400M Wing Attachment Frames, Proceedings of the 25th ICAF Symposium (2009)
- [2] Abaqus Analysis User's Manual, Version 6.17, Dassault Systèmes Simulia Corp.